Hindawi
Advances in Materials Science and Engineering
Volume 2022, Article ID 1898124, 15 pages
https://doi.org/10.1155/2022/1898124

Research Article

Investigation of Nonlinear Vibrational Analysis of Circular Sector Oscillator by Using Cascade Learning

Naveed Ahmad Khan,[1] **Muhammad Sulaiman**,[1] **Jamel Seidu**,[2] **and Fahad Sameer Alshammari**[3]

[1]*Department of Mathematics, Abdul Wali Khan University, Mardan 23200, Pakistan*
[2]*School of Railways and Infrastructure Development, University of Mines and Technology (UMaT) Essikado, Sekondi-Takoradi, Ghana*
[3]*Department of Mathematics, College of Science and Humanitiesin Alkharj, Prince Sattam Bin Abdulaziz University, Al-Kharj 11942, Saudi Arabia*

Correspondence should be addressed to Jamel Seidu; jseidu@umat.edu.gh

Received 28 May 2022; Accepted 8 August 2022; Published 5 September 2022

Academic Editor: Liancheng Zhao

This paper analyzed the model of swinging oscillation of a solid circular sector arising in hydrodynamical machines, electrical engineering, heat transfer applications, and civil engineering. Nonlinear differential equations govern the mathematical model for frequency oscillation of the system. Furthermore, a computational strength of Cascade neural networks (CNNs) is utilized with backpropagated Levenberg–Marquardt (BLM) algorithm to study the oscillations in angular displacement (θ), velocity (θ'), and acceleration (θ''). A data set for the supervised learning of the CNN-BLM algorithm for different angles (α) and radius (R) are generated by Runge–Kutta (RK-4) method. The BLM algorithm further interprets the dataset with log-sigmoid as an activation function for the solutions' validation, testing, and training. The results obtained by the design scheme are compared with Akbari–Ganji's (AG) method. The rapid convergence and quality of the solutions are validated through performance indicators such as mean absolute deviations (MAD), root means square error, and error in Nash–Sutcliffe efficiency (ENSE). The statistics demonstrate the design scheme's applicability and efficiency to highly singular nonlinear problems.

1. Introduction

Nonlinear oscillation and its behavior is an important topic in applied physics, mathematics, and mechanical engineering that has piqued the interest of many scientists from the dawn of human recognition of the equations of motion [1]. In vibrations theory, an extremely unique and important place is held by oscillatory systems that contain fundamental nonlinearities. On the other hand, it is of the utmost significance to comprehend their behavior, not only from an academic standpoint but also in view of the countless potential applications [2–4]. The systems of complex nonlinear and chaotic responses are characterized by a unique equilibrium position, a strong nonlinearity described by a monotone increasing mooring restoring force, and a fluid structure [5–7]. The dynamical systems, including spherical pendulum, harmonic oscillator model of aromaticity, spring systems, symmetric, and biased hardening duffing oscillators, produce the nonlinear and modulated responses of multidegree exhibits the periodic vibration, saturation, thermal resonance, and waves [8, 9]. Fox and Goulbourne [10, 11] carried out experiments to study primary and superharmonic resonances on the nonlinear oscillation of dielectric elastomers subjected to applied static pressure and dynamic voltage. A. Alibakhshi [12] investigated the static and dynamic response of the free and forced vibrations of a micro/nanobeam made of a hyperelastic material incorporating strain-stiffening, size effect, and moderate rotation.

The oscillation of a rigid rod over a circular surface is considered a classical oscillator whose mathematical model was first investigated by Gaylord [13] in 1979. Nonlinearity is an inherent property of every differential equation that describes a physical or biological phenomenon. Solving linear differential equations is quite straightforward and has been successfully implemented. On the other hand, the methods for solving nonlinear differential equations (NDEs) are not as readily available. Generally, NDEs do not have a precise solution. In general, finding exact and semianalytical solutions for such problems is challenging because of the nonlinearity in the elastic and damping components of the governing equations (14). NDEs have been the subject of all-embracing studies in various branches of nonlinear science and engineering. Poincare and Lyaponuv [15] were credited for being the first to solve the differential equations governing nonlinear processes. Their approaches were based on the existence of a values (large or small) parameter in the nonlinear equations, which allows the solution to be expanded as a power series whose components are generated by the integer powers of that small parameter. Using the series in the nonlinear model and equating the coefficients of the small parameters with like powers results in a system of linear ordinary differential equations whose solution caused the final result of the governing equation in closed form. This basic concept allowed the research community to solve numerous nonlinear scientific problems with a small or large parameter. The procedure was named the perturbation method. The method's only flaw is that it requires the existence of a small parameter in the equations, even though we know that the proposed parameter does not exist in many types of differential equations. A series of analytical and semiexact techniques that do not require a small parameter was proposed in the middle of the twentieth century to overcome the problem. Some well-known techniques used for the numerical and analytical solution of nonlinear problems are Adomian decomposition method (ADM) [16, 17], energy balance method (EBM) [18], variational iteration method (VIM) [19–21], extended direct algebraic method (EDAM) [22], Adams–Bashforth method [23], differential transform method [24], Hamiltonian approach [25, 26], Backlund method [27] rational harmonic balance method [28], min-max approach (MMA) [29, 30], power series technique [31], one-step hybrid block method [32], amplitude-frequency formulation (AFF) [33, 34], and modified homotopy perturbation method (MHPM) [35–37]. Ebrahimi Khah [38] studied the motion of a rigid rod rocking back over a circular surface using He's energy balance method. Galerkin method and modal analysis technique is utilized by G. Sheng [39, 40] to study the dynamic stability and nonlinear vibrations of the stiffened functionally graded (FG) cylindrical shell in a thermal environment. Reference [41] investigates the vibration analysis of a rigid rod using the Hamiltonian approach. Abul-Ez [42] employed the hybridization of the iteration perturbation method and variational iteration method to study the duffing oscillation of nonlinear oscillators. The above-cited literature shows that all of these techniques have been effectively applied to study the solutions and behavior of the nonlinear oscillatory models, but besides their advantages, it is observed with keen interest that such methods are gradient-based and require prior information about the problem. Prior information includes the choice of a small parameter, initial guess, continuity, and differentiability of the function. To overcome these drawbacks, gradient-free stochastic computing techniques based on the approximation ability of artificial neural networks are designed.

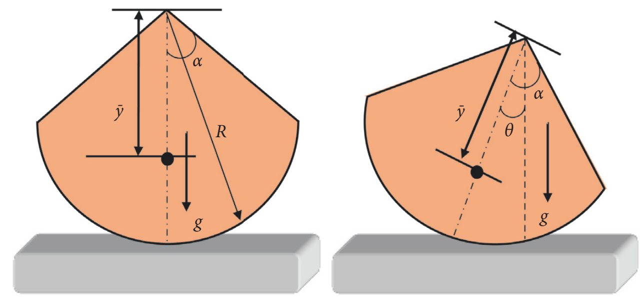

Figure 1: Geometric interpretation of a homogenous circular sector object over a solid surface.

The researcher's community has been widely employing the concepts of artificial neural network-based numerical computing techniques for exploring and exploiting linear/nonlinear mathematical systems. Some recent applications of the black-box stochastic methodologies include the approximate solutions for a mathematical model of chaotic base secure communication systems [43], nonlinear problems arising in heat transfer [44], thermal radiations of nanofluid [45, 46], nonlinear restoring moment and damping effects of ships [47], and wire coating dynamics [48]. These reported articles motivate authors to utilize the computational strength of artificial neural networks (ANNs) for the numerical treatment and analysis of nonlinear oscillation over a circular sector. The innovative insights of the presented study are summarized as follows:

(i) A mathematical model for the oscillation of a homogenous solid circular sector object is analyzed to study the influence of variations in angles and radius on angular frequency, velocity, and acceleration.

(ii) A novel application of artificial intelligence-based cascade neural networks via backpropagated Levenberg–Marquardt algorithm is presented effectively for the numerical solution of the nonlinear oscillator.

(iii) Approximate solutions for different scenarios of the nonlinear problem obtained by the design CNN-BLM algorithm are compared with analytical solutions by Ranga–Kutta method and Akbari–Ganji's method.

(iv) The proposed algorithm is executed multiple times to test the results' convergence, accuracy, and effectiveness. The performance of CNN-BLM is further validated by mean absolute deviations (MAD), root means square errors, and errors in Nash–Sutcliffe efficiency (ENSE).

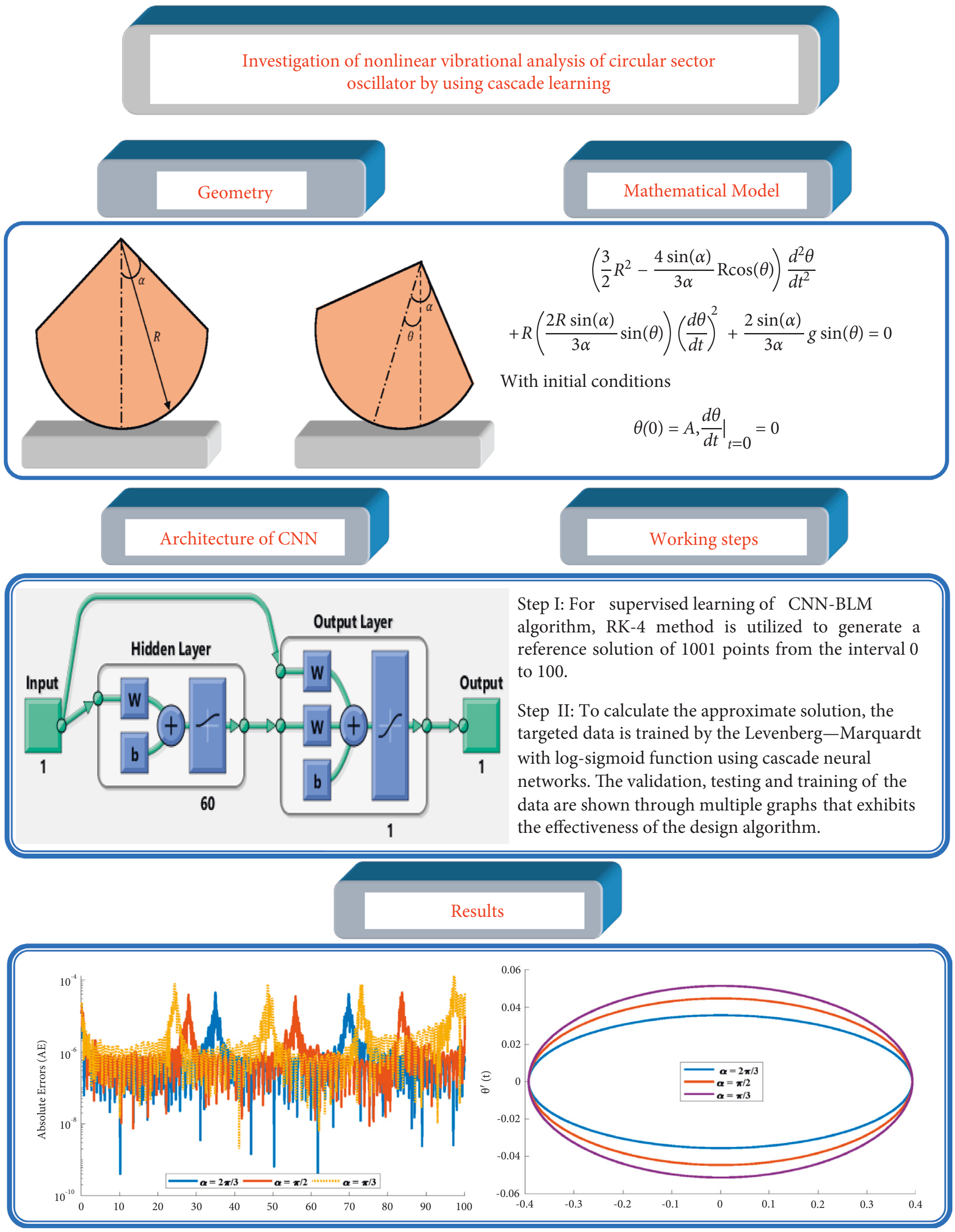

FIGURE 2: A detailed graphical illustration of the physical problem with its mathematical model, the solution strategy based on the architecture of cascade learning, and the optimization framework of the Levenberg–Marquardt algorithm to measure the influence of R and α on displacement, velocity, and acceleration of the circular sector.

2. Swinging Oscillation of a Solid Circular Sector Object

In this section, an oscillation of homogenous circular sector of angle α and radius (R) over a solid surface is considered as shown in Figure 1. The circular object is allowed to roll on a fixed solid surface producing an oscillatory motion (back and forth) with no sliding effect, it is evident that α will

TABLE 1: Different cases of equation (3) based on variations in radius and angular displacement of a circular sector with $A = \pi/8$ and $g = 9.8\,\mathrm{ms}^{-2}$.

Angular displacement				
Scenarios	Radius	Case I	Case II	Case III
1	15	$\alpha = 2\pi/3$	$\alpha = \pi/2$	$\alpha = \pi/3$
2	10	$\alpha = 2\pi/3$	$\alpha = \pi/2$	$\alpha = \pi/3$
3	05	$\alpha = 2\pi/3$	$\alpha = \pi/2$	$\alpha = \pi/3$

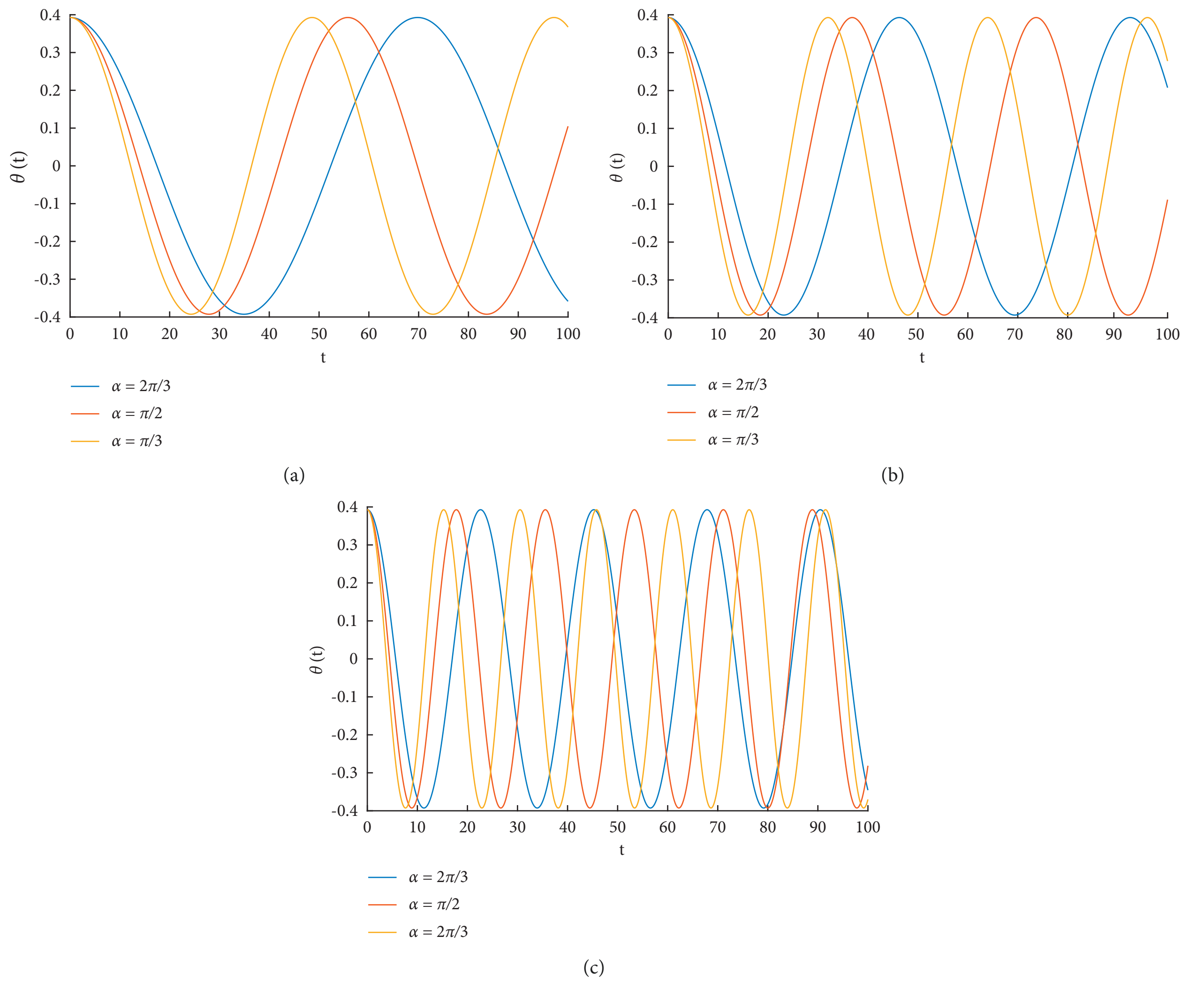

Figure 3: Influence of variations in R and α on an angular displacement of a circular sector.

Table 2: Comparison of approximate solutions obtained by the proposed algorithm for the influence of variations in α with $R = 15$ on an angular displacement of a homogenous circular sector.

	Case I			Case II			Case III		
t	Numerical	AGM	CNN-BLMA	Numerical	AGM	CNN-BLMA	Numerical	AGM	CNN-BLMA
0	0.39269908	**0.39269908**	0.392687276	0.39269908	**0.39269908**	0.392686548	0.39269908	**0.39269908**	0.392681150
10	0.24512253	0.24501045	**0.245122185**	0.17012305	0.16964486	**0.170122142**	0.10875275	0.10762438	**0.108752428**
20	−0.08993096	0.09371990	**−0.089931250**	−0.24887845	−0.25944763	**−0.248879413**	−0.33471506	−0.35104698	**−0.334714661**
30	−0.35555274	0.36692738	**−0.355552929**	−0.38187454	−0.38749464	**−0.381874167**	−0.29201803	−0.27870234	**−0.292017486**
40	−0.35254525	0.35162485	**−0.352544182**	−0.08143699	−0.05286683	**−0.081436623**	0.17597552	0.20864948	**0.175975984**
50	−0.08307460	0.06065639	**−0.083074398**	0.31332380	0.33172291	**0.313323484**	0.38631310	0.37789019	**0.386315754**
60	0.25054818	0.26978783	**0.250548338**	0.34991634	0.33408668	**0.349915015**	0.03769972	−0.00330218	**0.037698188**
70	0.39263866	0.39135302	**0.392621108**	−0.01205181	−0.04827707	**−0.012052894**	−0.36626688	−0.39470691	**−0.366268070**
80	0.23961867	0.21847002	**0.239617147**	−0.36004875	−0.38611530	**−0.360049029**	−0.23945080	−0.18427538	**−0.239449924**
90	−0.09675804	−0.12620233	**−0.096759026**	−0.29838583	−0.26304319	**−0.298385305**	0.23706674	0.29236833	**0.237067580**
100	−0.35844921	−0.37955984	**−0.358447834**	0.10482796	0.16555209	**0.104818684**	0.36732664	0.33439609	**0.367367867**

change, and the system will satisfy the following nonlinear differential equation [49, 50]:

$$\left(\frac{3}{2\lambda} - 2\cos(\theta)\right)\theta + \sin(\theta)\dot{\theta}^{2} + \frac{\lambda g}{R}\sin(\theta) = 0. \tag{1}$$

Introducing the dimensionless geometrical parameter

$$\lambda = \frac{\overline{y}}{R} = \frac{2\sin(\alpha)}{3\alpha}, \tag{2}$$

Table 3: Comparison of approximate solutions obtained by the proposed algorithm for different cases of scenarios 2 and 3 of angular displacement of a homogenous circular sector.

	Case I		Case II		Case III		Case I		Case II		Case III	
t	Numerical	CNN-BLMA	Numerical	CNN-BLMA	Numerical	CNN-BLMA	Numerical	CNN-BLMA	Numerical	CNN-BLMA	Numerical	CNN-BLMA
0	0.392699082	0.392685093	0.392699082	0.392670786	0.392699082	0.392661944	0.39269908	0.392624275	0.39269908	0.39259210	0.39269908	0.39256229
10	0.083388890	0.083389783	−0.053232122	−0.053235250	−0.151961836	−0.151961785	−0.36749090	−0.367653662	−0.36374462	−0.36345803	−0.22287067	−0.22264354
20	−0.358208978	−0.358210302	−0.378788375	−0.378796623	−0.278995466	−0.279004381	0.29461331	0.294685021	0.28024739	0.28022323	−0.14975320	−0.14978926
30	−0.234800091	−0.234800409	0.155649427	0.155648690	0.363640049	0.363652579	−0.18251243	−0.182477435	−0.15297185	−0.15299577	0.38443195	0.38481916
40	0.260262179	0.260262109	0.337907757	0.337907826	−0.000819025	−0.000819677	0.04540274	0.045441209	0.00077900	0.00061557	−0.28550774	−0.28569189
50	0.343613202	0.343612501	−0.246351630	−0.246347082	−0.363030749	−0.363041240	0.09803384	0.098023706	0.15154292	0.15147925	−0.06938614	−0.06961510
60	−0.115291291	−0.115290537	−0.272637949	−0.272634926	0.280132157	0.280142714	−0.22786478	−0.227850757	−0.27917225	−0.27905960	0.35986908	0.35952351
70	−0.391351734	−0.391304302	0.318824563	0.318825376	0.150454989	0.150457157	0.32678376	0.326762802	0.36317118	0.36298554	−0.33516516	−0.33536112
80	−0.050882422	−0.050882087	0.187321504	0.187318255	−0.392695353	−0.392577931	−0.38266277	−0.382575699	−0.39269606	−0.39197161	0.01440356	0.01442215
90	0.370322679	0.370323421	−0.368151155	−0.368156176	0.153465671	0.153473754	0.38920766	0.389280863	0.36431245	0.36406319	0.31975532	0.32062675
100	0.207666340	0.207662784	−0.087977218	−0.087990333	0.277853197	0.278105162	−0.34571116	−0.345711854	−0.28131805	−0.28162897	−0.37007441	−0.37007000

Table 4: Comparison of absolute errors in solutions obtained by CNN-BLM algorithm with Akbari–Ganji's method for different scenarios of equation (3).

Scenario 1							Scenario 2			Scenrio 3		
	Case I		Case II		Case III		Case I	Case II	Case III	Case I	Case II	Case III
t	AGM	CNN-BLMA	AGM	CNN-BLMA	AGM	CNN-BLMA	CNN-BLMA	CNN-BLMA	CNN-BLMA	CNN-BLMA	CNN-BLMA	CNN-BLMA
0	$0.00E+00$	$1.18E-05$	$0.00E+00$	$1.25E-05$	$0.00E+00$	$1.79E-05$	$1.40E-05$	$2.83E-05$	$3.71E-05$	$7.48E-05$	$1.07E-04$	$1.37E-04$
10	$1.12E-04$	$\mathbf{1.36E-07}$	$4.78E-04$	$\mathbf{6.49E-07}$	$1.13E-03$	$\mathbf{1.42E-08}$	$8.93E-07$	$3.13E-06$	$5.09E-08$	$1.63E-04$	$2.87E-04$	$2.27E-04$
20	$3.79E-03$	$\mathbf{9.30E-08}$	$1.06E-02$	$\mathbf{6.91E-07}$	$1.63E-02$	$\mathbf{6.06E-07}$	$1.32E-06$	$8.25E-06$	$8.92E-06$	$7.17E-05$	$2.42E-05$	$3.61E-05$
30	$1.14E-02$	$\mathbf{3.35E-07}$	$5.62E-03$	$\mathbf{3.73E-07}$	$1.33E-02$	$\mathbf{1.38E-07}$	$3.18E-07$	$7.37E-07$	$1.25E-05$	$3.50E-05$	$2.39E-05$	$3.87E-04$
40	$9.20E-04$	$\mathbf{5.13E-07}$	$2.86E-02$	$\mathbf{3.39E-07}$	$3.27E-02$	$\mathbf{2.49E-07}$	$7.00E-08$	$6.93E-08$	$6.52E-07$	$3.85E-05$	$1.63E-04$	$1.84E-04$
50	$2.24E-02$	$\mathbf{2.57E-07}$	$1.84E-02$	$\mathbf{5.25E-07}$	$8.42E-03$	$\mathbf{2.98E-06}$	$7.01E-07$	$4.55E-06$	$1.05E-05$	$1.01E-05$	$6.37E-05$	$2.29E-04$
60	$1.92E-02$	$\mathbf{2.99E-07}$	$1.58E-02$	$\mathbf{6.24E-07}$	$4.10E-02$	$\mathbf{5.34E-07}$	$7.54E-07$	$3.02E-06$	$1.06E-05$	$1.40E-05$	$1.13E-04$	$3.46E-04$
70	$1.29E-03$	$\mathbf{1.67E-05}$	$3.62E-02$	$\mathbf{6.55E-08}$	$2.84E-02$	$\mathbf{1.33E-06}$	$4.74E-05$	$8.13E-07$	$2.17E-06$	$2.10E-05$	$1.86E-04$	$1.96E-04$
80	$2.11E-02$	$\mathbf{5.31E-07}$	$2.61E-02$	$\mathbf{3.25E-07}$	$5.52E-02$	$\mathbf{4.38E-07}$	$3.35E-07$	$3.25E-06$	$1.17E-04$	$8.71E-05$	$7.24E-04$	$1.86E-05$
90	$2.94E-02$	$\mathbf{7.00E-07}$	$3.53E-02$	$\mathbf{7.83E-07}$	$5.53E-02$	$\mathbf{5.88E-07}$	$7.42E-07$	$5.02E-06$	$8.08E-06$	$7.32E-05$	$2.49E-04$	$8.71E-04$
100	$2.11E-02$	$\mathbf{5.37E-07}$	$6.07E-02$	$\mathbf{9.28E-06}$	$3.29E-02$	$\mathbf{4.26E-05}$	$3.56E-06$	$1.31E-05$	$2.52E-04$	$6.99E-07$	$3.11E-04$	$1.92E-06$

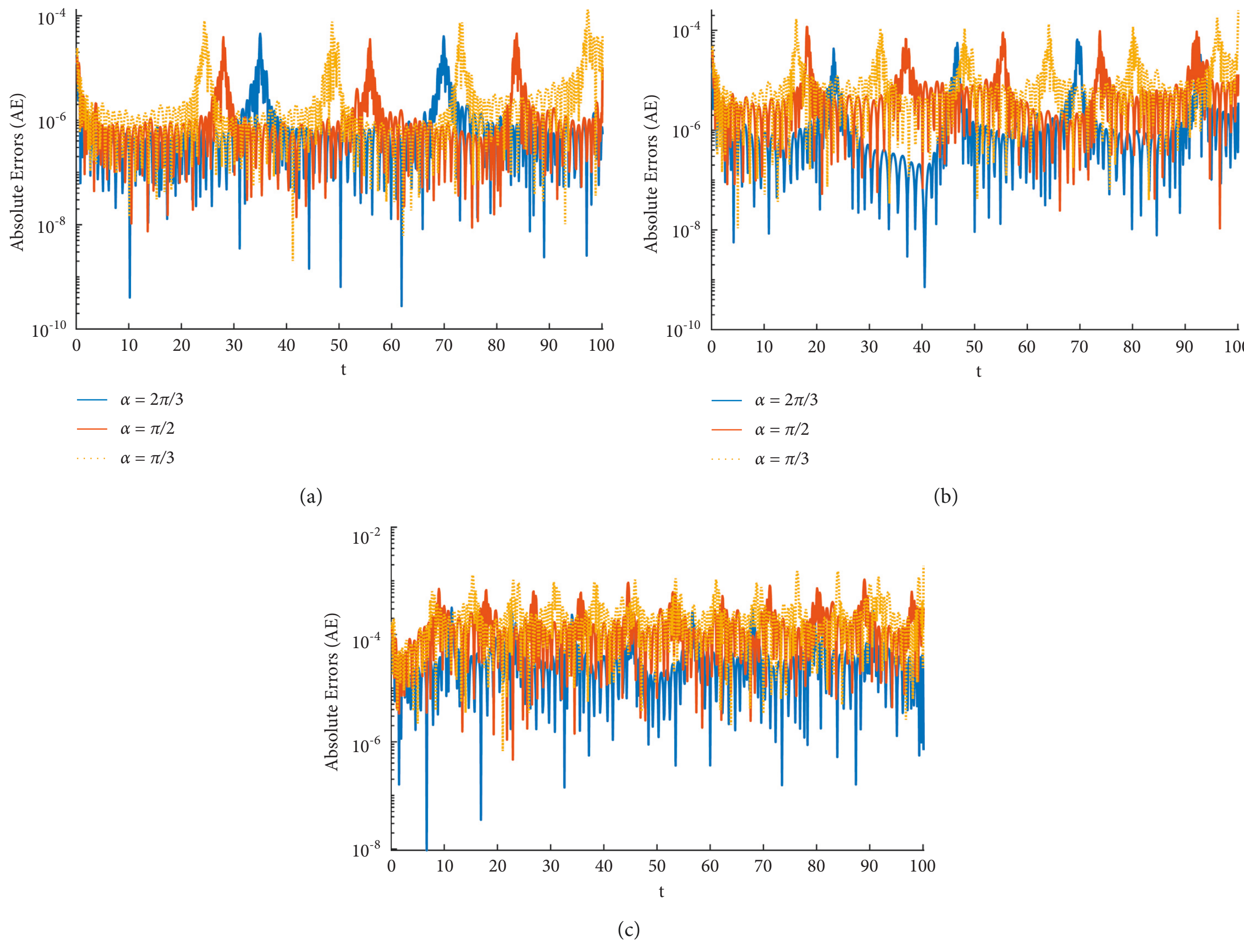

FIGURE 4: Absolute errors in solutions of CNN-BLM algorithm for different cases of scenarios 1, 2, and 3.

where $\overline{y} = 2R\sin(\alpha)/3\alpha$ is the height of the mass center. Using (2) in (1) will give

$$\left(\frac{3}{2}R^2 - \frac{4\sin(\alpha)}{3\alpha}R\cos(\theta)\right)\frac{d^2\theta}{dt^2} + R\left(\frac{2R\sin(\alpha)}{3\alpha}\sin(\theta)\right)\left(\frac{d\theta}{dt}\right)^2 + \frac{2\sin(\alpha)}{3\alpha}g\sin(\theta) = 0. \tag{3}$$

Subjected to the initial conditions

$$\theta(0) = A, \left.\frac{d\theta}{dt}\right|_{t=0} = 0, \tag{4}$$

where A is vibrational amplitude, θ denotes the angular displacement, and t is the dimensionless time variable.

3. Design Methodology

3.1. Cascade Neural Networks. An artificial neural network (ANN) is a collection of interconnected, basic components known as neurons with multiple inputs and a single output, and each neuron represents a mapping. The output of a neuron is a function of the sum of its inputs which is generated with the help of the activation function. A neural network architecture that only contains the input and output layer is called perceptron [51]. The sum of weighted signals in perceptron is transmitted directly to the output layer from the input layer. In neural network modeling, multilayer perceptron (MLP), also called feed-forward neural network (FNN) comes with an additional layer between the input and output layer known as the hidden layer. In MLP, the signals that enter the hidden layer are processed by the transfer function to obtain the desired results. In FNN, the connection between the input and output layer is indirect while in perceptron, they possess a direct relation. The direct network between input and output layers formulated by the combination of MLP and perceptron is named as cascade neural networks (CNNs) [52]. The basic structure of CNN is based on two ideas. First, is to build an architecture of cascade by adding new neurons with their connection to all inputs and previously hidden neurons without changing configuration at each layer. The second idea is to minimize the residual error by training only the newly created neurons by fitting their weights. The network is updated with new neurons and the performance increases.

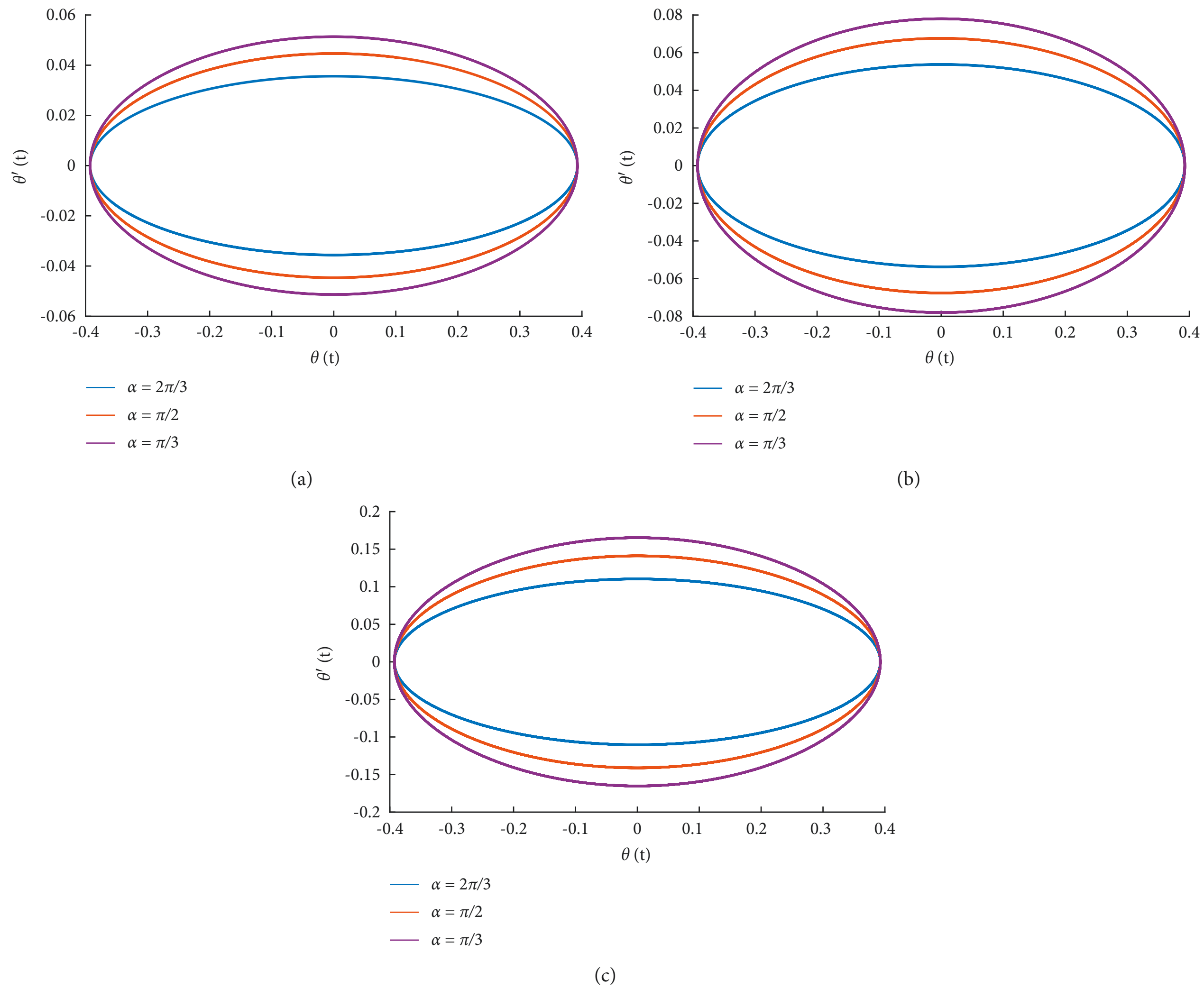

Figure 5: Stability analysis in terms of angular velocity and acceleration by CNN-BLM algorithm for different cases of scenarios 1, 2, and 3.

Initially, the cascade neural networks start the process with m inputs and a single targeted date without hidden neurons. The output neuron is connected to each input using weights such as $(w_1, w_2 \ldots, w_m)$ with a standard sigmoid function. The Log-sigmoid is one of the best nonlinear normalized functions, which is differentiable and continuous; therefore, it gives a smooth gradient preventing jumps in the output values. The output of the network is presented as

$$y = f(\mathbf{x}; \mathbf{w}) = \frac{1}{\left(1 + \exp\left(-w_0 - \sum_i^m w_i x_i\right)\right)}. \qquad (5)$$

The new neurons formed are added to the network, and each neuron is connected to hidden neurons. A suitable algorithm trains the neurons for output. The basic advantage of CNN is that no structure for the network is predefined, it automatically built its architecture from the training data. Secondly, the learning process of CNN is fast compared to other networks because each neuron is trained independently.

3.2. Learning Procedure and Performance Measures. This section discusses the working and training procedure of neurons in CNN architecture. The learning strategy of the neurons in CNN is based on two phases. Initially, a network is presented with inputs of the reference data set of 1001 points generated by the Ranka–Kutta method. Secondly, the inputs and the weights in CNN are trained by an appropriate algorithm Levenberg–Marquardt with a log-sigmoid activation function for the output. The architecture of CNN along with the workflow of the design algorithm is shown in Figure 2.To examine the accuracy and effectiveness of the results of the CNN-BLM algorithm for oscillations of the nonlinear circular sector, performance indices are defined in terms of mean square error (MSE) of fitness function of the model, regression R^2, absolute errors (AE), mean absolute deviations (MAD), root mean square error (RMSE), and error in Nash–Sutcliffe efficiency (ENSE). Formulation of these indices is given as [53]

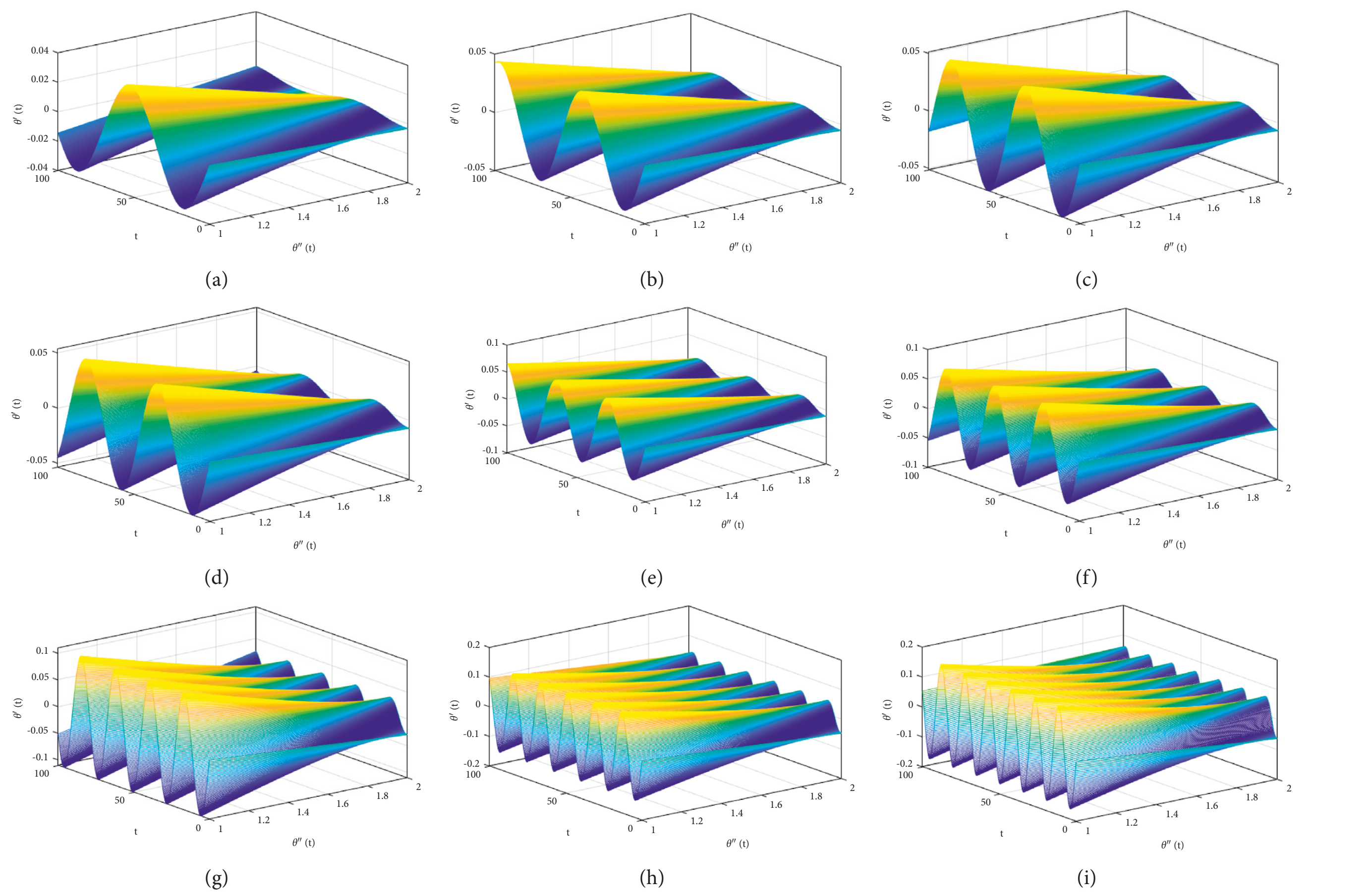

Figure 6: Surface plots for the comparison of angular velocity and acceleration of different cases and scenarios of oscillation in the homogenous circular sector.

$$\begin{aligned}
\text{MSE} &= \frac{1}{k}\sum_{j=1}^{k}\left(\theta_j(t)-\widehat{\theta}_j(t)\right)^2,\\
R^2 &= 1-\frac{\sum_{j=1}^{k}\left(\widehat{\theta}_j(t)-\overline{\theta}_j(t)\right)^2}{\sum_{j=1}^{k}\left(\theta_j(t)-\overline{\theta}_j(t)\right)^2},\\
\text{AE} &= \left|\theta_j(t)-\overline{\theta}_j(t)\right|,\\
\text{MAD} &= \frac{1}{k}\sum_{m=1}^{n}\left|\theta_j(t)-\overline{\theta}_j(t)\right|,\\
\text{NSE} &= \left\{1-\frac{\sum_{j=1}^{k}\left(\theta_j(t)-\overline{\theta}_j(t)\right)^2}{\sum_{j=1}^{k}\left(\left(\theta_j(t)-\widehat{\theta}_j(t)\right)\right)^2},\widehat{\theta}(x)=\frac{1}{k}\sum_{j=1}^{k}\theta_j(t),\right.\\
ENSE &= 1-NSE,
\end{aligned} \tag{6}$$

here, n shows the number of grid points, θ_j, $\overline{\theta}_j$ and $\widehat{\theta}_j$ are the reference, approximate, and mean of solution at jth input. The desired value of MSE, AE, MAD, RMSE, and ENSE for perfect fitting is equal to zero while the value of R^2 and NSE should be one.

4. Numerical Experimentation and Discussion

In this section, the artificial intelligence-based stochastic numerical technique is implemented on a nonlinear mathematical model of oscillations in a circular section given by equations (3)–(4) to study the angular displacement, velocity, and acceleration. Different cases of the problem based on variations in R and α are given in Table 1.

Approximate solutions for angular displacement of solid circular sector obtained by the designs scheme for different values of radius and angle are shown in Figure 3. It can be seen that by reducing the angle with a constant semicircular radius, the frequency of oscillation increases. Also, reducing the semicircular radius R causes an increase in the frequency of the oscillation. It is worthy to note that the frequency of oscillation determined by the design scheme is higher than the frequency obtained by Akbari–Ganji's (AG) method for different cases of scenario 1 as shown in Table 2. Table 3 compares the proposed algorithm's approximate solutions with numerical solutions by the RK-4 method. Results of CNN-BLM for different scenarios of (3) overlap the analytical solution with minimum absolute errors, as shown in Table 4.

Table 5: Statistics of performance function in terms of mean square error for the influence of variations in R and α in equation (3).

R	Case I			Case II			Case III		
	Min	Mean	Std	Min	Mean	Std	Min	Mean	Std
15	$3.60E-12$	$1.05E-09$	$2.15E-09$	$1.54E-11$	$1.16E-10$	$2.57E-10$	$1.04E-10$	$3.67E-10$	$3.05E-10$
10	$3.00E-11$	$2.03E-10$	$2.13E-10$	$2.07E-10$	$1.09E-09$	$1.97E-09$	$3.67E-10$	$3.32E-09$	$7.16E-09$
5	$3.52E-09$	$1.80E-08$	$3.31E-08$	$5.26E-08$	$2.56E-07$	$6.29E-07$	$1.17E-07$	$5.06E-07$	$8.12E-07$

Table 6: Results of the gradient in terms of minimum, the mean, and standard deviation for different cases and scenarios of the problem.

R	Case I			Case II			Case III		
	Min	Mean	Std	Min	Mean	Std	Min	Mean	Std
15	$2.77E-09$	$2.77E-09$	$9.86E-07$	$6.52E-10$	$3.30E-08$	$7.88E-08$	$2.86E-09$	$5.91E-08$	$1.84E-07$
10	$4.94E-09$	$1.90E-07$	$2.99E-07$	$4.34E-09$	$2.51E-07$	$6.01E-07$	$3.63E-09$	$2.14E-07$	$6.84E-07$
5	$2.19E-08$	$2.95E-07$	$4.62E-07$	$2.28E-08$	$3.10E-07$	$4.53E-07$	$7.90E-09$	$3.52E-07$	$5.46E-07$

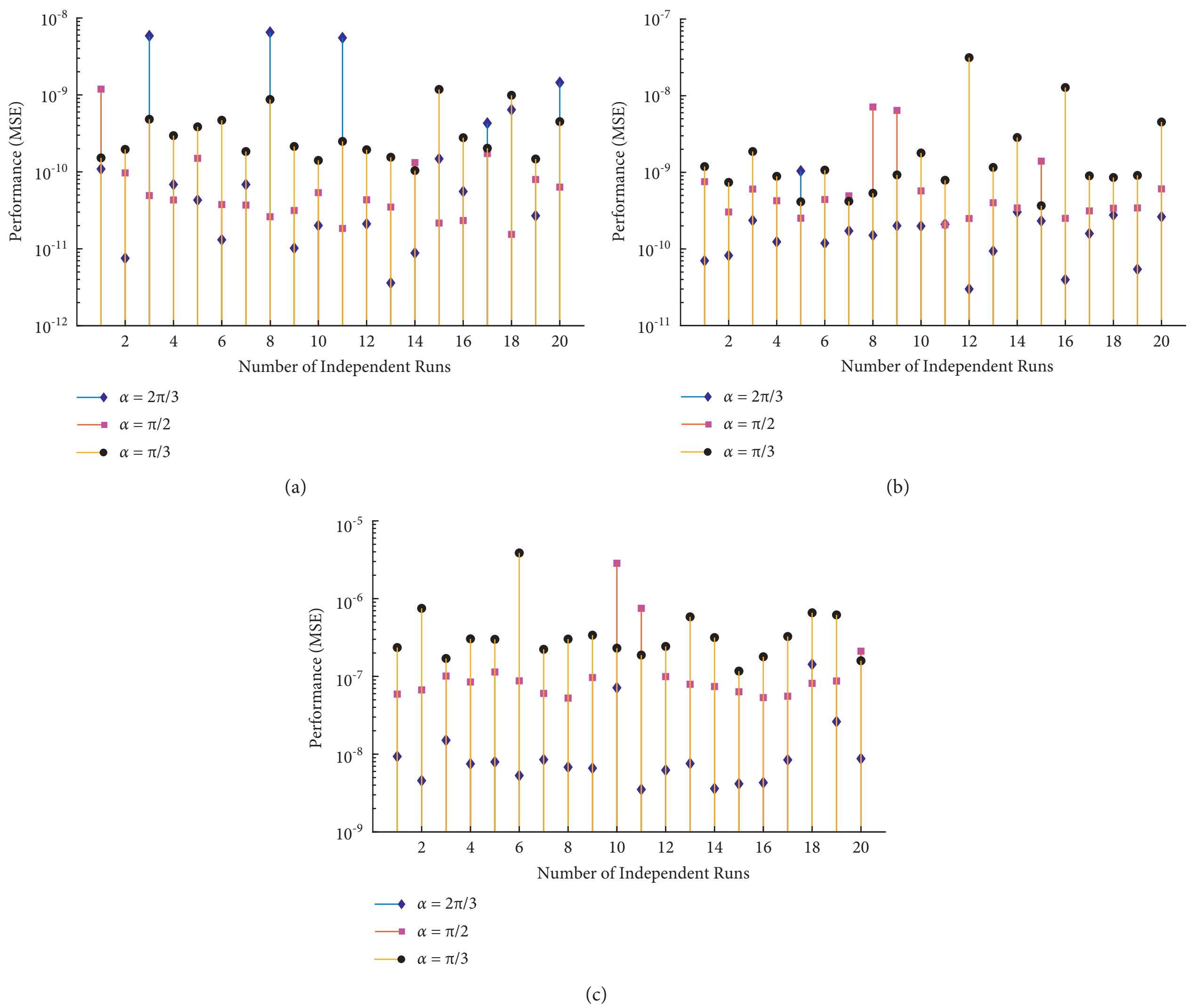

Figure 7: Values of performance function in terms of mean square error for different scenarios and cases of equation (3).

To study the smoothness of solutions, absolute errors for 1001 points are plotted in Figure 4. For scenario 1, the mean values of absolute errors lie around 10^{-6} to 10^{-9} while the maximum values of absolute errors lie around 10^{-4} to 10^{-5} at $t = 25, 30, 35, 50, 70, 85$ and 100. Similarly, the mean absolute errors for scenario 2 and 3 lies around 10^{-5} to 10^{-8}

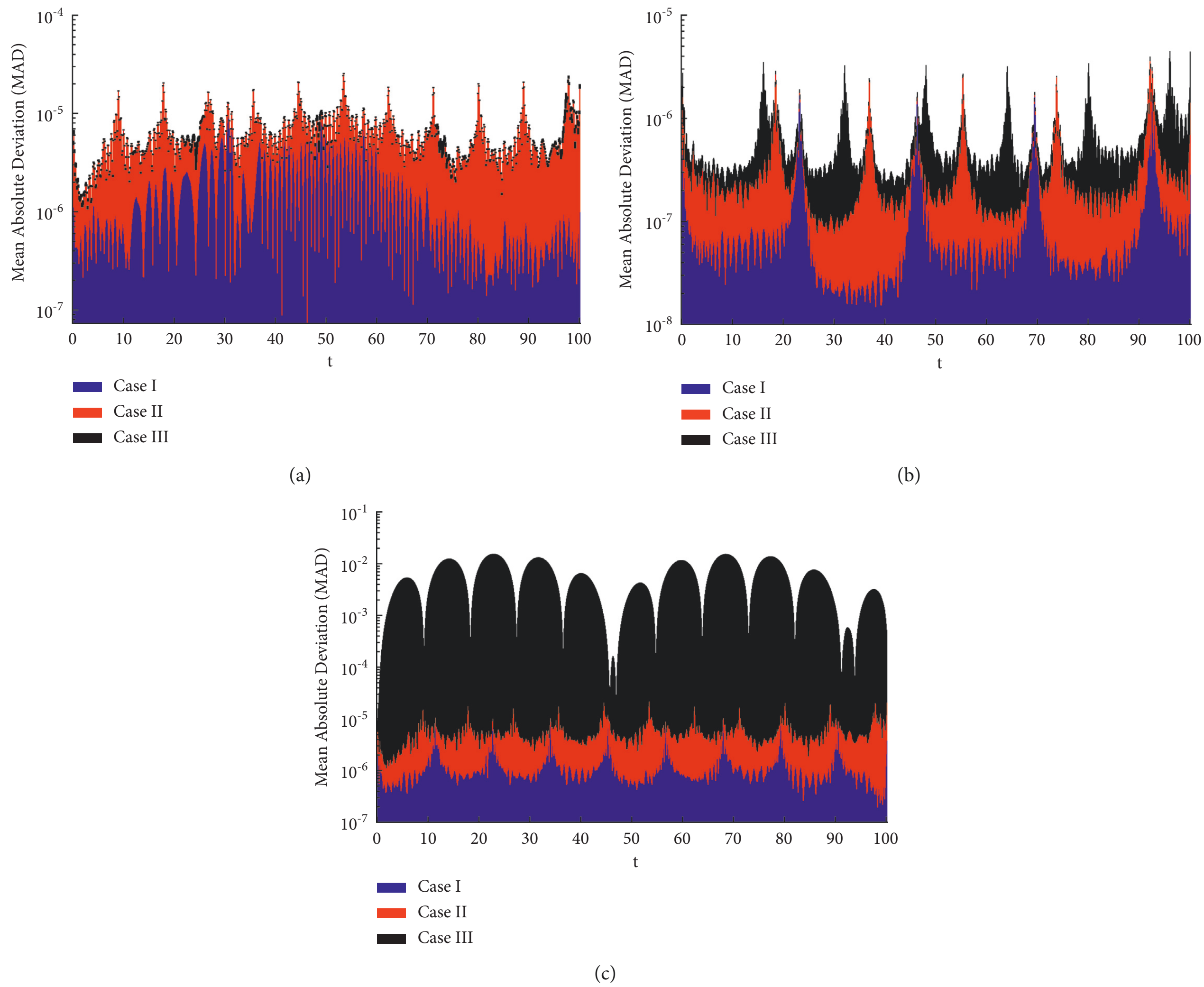

Figure 8: Behavior of values of mean absolute deviations for different scenarios and cases of equation (3).

Table 7: Statistics of root mean square error in our solutions for different cases and scenarios of the homogenous circular sector.

R	Case I			Case II			Case III		
	Min	Mean	Std	Min	Mean	Std	Min	Mean	Std
15	$1.01E-06$	$4.74E-05$	$5.26E-05$	$6.24E-06$	$5.27E-05$	$3.25E-05$	$1.55E-07$	$1.07E-06$	$1.80E-06$
10	$1.24E-07$	$1.02E-06$	$1.52E-06$	$4.10E-07$	$2.35E-06$	$2.69E-06$	$5.69E-07$	$3.70E-06$	$4.45E-06$
5	$1.63E-06$	$1.17E-05$	$9.40E-06$	$6.24E-06$	$5.27E-05$	$3.25E-05$	$3.06E-05$	$4.33E-03$	$3.24E-03$

Table 8: Results of ENSE obtained by the design scheme during 20 independent runs.

R	Case I			Case II			Case III		
	Min	Mean	Std	Min	Mean	Std	Min	Mean	Std
15	$7.46E-11$	$7.52E-08$	$1.41E-07$	$6.79E-09$	$4.11E-07$	$7.57E-07$	$3.84E-12$	$8.45E-10$	$4.52E-09$
10	$7.21E-09$	$5.60E-06$	$5.25E-05$	$3.03E-11$	$1.86E-09$	$8.37E-09$	$4.83E-11$	$4.42E-09$	$1.65E-08$
5	$5.18E-10$	$3.57E-08$	$9.72E-08$	$5.18E-10$	$3.57E-08$	$9.72E-08$	$2.00E-08$	$1.22E-04$	$5.97E-04$

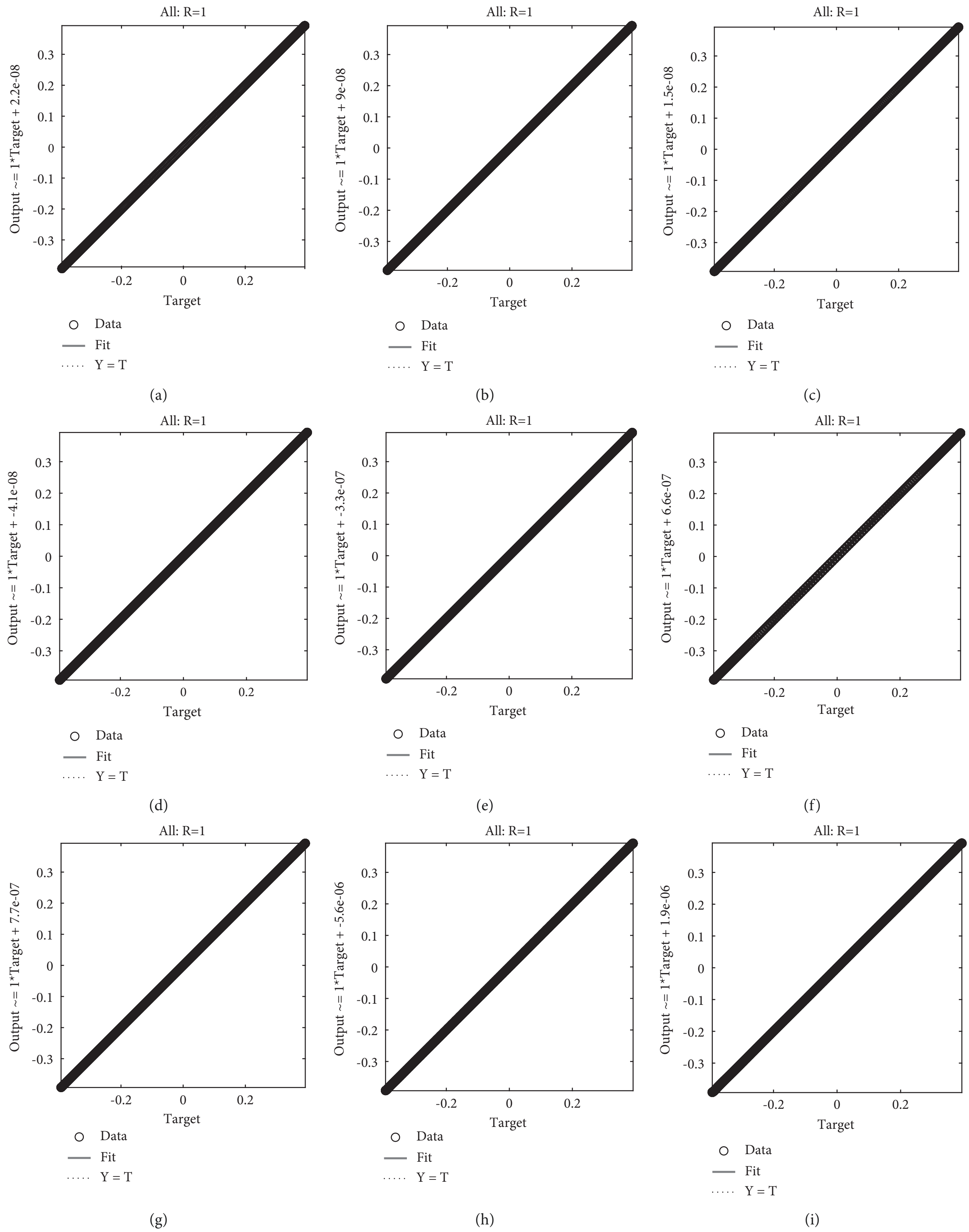

Figure 9: Regression analysis for each case of scenarios 1, 2, and 3 of a homogenous circular sector.

and 10^{-4} to 10^{-7}, respectively. Furthermore, to study the angular displacement and velocity, graphs of θ against θ' are shown though Figure 5. Apart from the graphs of the solutions, Figure 5 depicts that the oscillation trends are somehow harmonic and stable. It can be seen that velocity reaches its peak when the angle (α) or semicircular (R) decreases. Surface plots are shown through Figure 6 for angular velocity and acceleration in the homogenous circular sector. The oscillations are all stable because neither successive increases in the amplitudes are noticed in the displacement time diagram, nor open curves have been detected in the phase plane.To study the performance of the design scheme, the CNN-BLM algorithm is executed for 20 independent runs. Results of performance function in terms of mean square errors are dictated in Tables 5 and 6 and plotted through Figure 7. Mean values of MSE lie around 10^{-7} to 10^{-10}. Figure 8 shows the convergence of mean absolute deviations of the solutions at each step size. It can be seen that the mean value of MAD for each case lies around 10^{-8} to 10^{-9}. Tables 7 and 8 dictates the statistics of root mean square error (RMSE) and error in Nash–Sutcliffe efficiency (ENSE) in terms of minimum, mean and standard deviations. Additionally, regression plots are shown in Figure 9. It can be seen that the values of regression for each case are equal to unity which shows the efficiency, correctness, and accuracy of the results obtained by the CNN-BLM algorithm for oscillations in the homogenous circular sector.

5. Conclusions

In this paper, an artificial intelligent strength of cascade neural networks with backpropagated Levenberg–Marquardt algorithm is utilized to study the swinging oscillation of a solid circular sector over a solid surface. The governing relation of the system was presented in the form of the differential equation. The proposed algorithm is implemented to study the effect of variations in semicircular radius R and semicircular angle (α) on angular displacement, velocity, and acceleration of the system. The results dictate that by reducing the angle with a constant semicircular radius, the frequency of oscillation increases, in these cases, higher velocities are achievable and the phase-plane ellipse height is greater. In addition, reducing the semicircular radius R also causes an increase in the frequency of the oscillation. The approximate solution for angular displacement obtained by the CNN-BLM algorithm is compared with analytical solutions and approximate solutions by Akbari–Ganji's (AG) method. Absolute errors demonstrate the effectiveness of the results as the solutions by the CNN-BLM algorithm overlap the numerical solution up to 8 and 9 decimal places. Statistics of MAD, RMSE, MSE, and ENSE lie between 10^{-5} to 10^{-6}, 10^{-6} to 10^{-7}, 10^{-9} to 10^{-12}, and 10^{-9} to 10^{-11} which reflects the accuracy of solutions and validates the worth, efficiency, and stability of the proposed algorithm.

In the future, the authors aim to implement cascade neural networks to study the solutions of nonlinear fractional differential equations modeling physical problems such as biochemical reactors, skin cancer, tumor growth, physiological temperature regulations, drying processes, and chaotic behaviors in warless communications.

Data Availability

The data that support the findings of this study are available from the corresponding author upon reasonable request.

Conflicts of Interest

The authors declare that they have no conflicts of interest.

Authors' Contributions

All authors equally contributed to this manuscript and approved the final version.

References

[1] A. Lashkarboluki, H. Hosseini, and D. D. Ganji, "Investigating the solutions of two classical nonlinear oscillators by the AG method," *International Journal of Algorithms, Computing and Mathematics*, vol. 7, no. 3, pp. 110–128, 2021.

[2] V. Arnold, "Variational principles," in *Mathematical Methods of Classical Mechanics*, pp. 55–74, Springer, Berlin/Heidelberg, Germany, 1989.

[3] Z. Shah, E. Bonyah, E. Alzahrani, R. Jan, and N. Aedh Alreshidi, "Chaotic phenomena and oscillations in dynamical behaviour of financial system via fractional calculus," *Complexity*, vol. 2022, Article ID 8113760, 14 pages, 2022.

[4] V. Babitsky, V. Krupenin, and J. Angeles, "Vibration of strongly nonlinear discontinuous systems. Foundations of engineering mechanics," *Applied Mechanics Reviews*, vol. 55, no. 4, pp. 65–B66, 2002.

[5] J. M. T. Thompson, "Complex dynamics of compliant offshore structures," *Proceedings of the Royal Society of London. A. Mathematical and Physical Sciences*, vol. 387, pp. 407–427, 1983.

[6] F. A. Papoulias and M. M. Bernitsas, "Autonomous oscillations, bifurcations, and chaotic response of moored vessels," *Journal of Ship Research*, vol. 32, no. 03, pp. 220–228, 1988.

[7] W. Szemplińska-Stupnicka and J. Bajkowski, "The subharmonic resonance and its transition to chaotic motion in a non-linear oscillator," *International Journal of Non-Linear Mechanics*, vol. 21, no. 5, pp. 401–419, 1986.

[8] J. W. Miles, "Stability of forced oscillations of a spherical pendulum," *Quarterly of Applied Mathematics*, vol. 20, no. 1, pp. 21–32, 1962.

[9] P. R. Sethna and A. K. Bajaj, "Bifurcations in dynamical systems with internal resonance," *Journal of Applied Mechanics*, vol. 45, no. 4, pp. 895–902, 1978.

[10] J. Fox and N. Goulbourne, "On the dynamic electromechanical loading of dielectric elastomer membranes," *Journal of the Mechanics and Physics of Solids*, vol. 56, no. 8, pp. 2669–2686, 2008.

[11] J. Fox and N. Goulbourne, "Electric field-induced surface transformations and experimental dynamic characteristics of dielectric elastomer membranes," *Journal of the Mechanics and Physics of Solids*, vol. 57, no. 8, pp. 1417–1435, 2009.

[12] A. Alibakhshi, S. Dastjerdi, M. Malikan, and V. A. Eremeyev, "Nonlinear free and forced vibrations of a hyperelastic

micro/nanobeam considering strain stiffening effect," *Nanomaterials*, vol. 11, p. 3066, 2021.
[13] A. H. Nayfeh, D. T. Mook, and P. Holmes, "Nonlinear oscillations," *Journal of Applied Mechanics*, vol. 47, no. 3, p. 692, 1980.
[14] D. Kumar, J. Singh, and D. Baleanu, "A hybrid computational approach for Klein–Gordon equations on Cantor sets," *Nonlinear Dynamics*, vol. 87, no. 1, pp. 511–517, 2017.
[15] A. M. Lyapunov and J. A. Walker, "The general problem of the stability of motion," *Journal of Applied Mechanics*, vol. 61, no. 1, pp. 226-227, 1994.
[16] G. Adomian, "Solving Frontier problems of physics: the decomposition method, with a preface by Yves Cherruault," *Fundamental Theories of Physics*, p. 1, Kluwer Academic Publishers Group, Dordrecht, 1994.
[17] M. Najafi, H. Massah, and M. Daemi, "On the application of Adomian decomposition method and oscillation equations," in *Proceedings of the 9th WSEAS International Conference on Applied Mathematics (MATH'06)*, Istanbul, Turkey, May 2006.
[18] J. H. He, "Preliminary report on the energy balance for nonlinear oscillations," *Mechanics Research Communications*, vol. 29, no. 2-3, pp. 107–111, 2002.
[19] J. H. He, "Variational iteration method–a kind of non-linear analytical technique: some examples," *International Journal of Non-Linear Mechanics*, vol. 34, no. 4, pp. 699–708, 1999.
[20] D. Younesian, Z. Saadatnia, and H. Askari, "Analytical solutions for free oscillations of beams on nonlinear elastic foundations using the variational iteration method," *Journal of Theoretical and Applied Mechanics*, vol. 50, pp. 639–652, 2012.
[21] S. Rehman, A. Hussain, J. U. Rahman, N. Anjum, and T. Munir, "Modified Laplace based variational iteration method for the mechanical vibrations and its applications," *Acta Mechanica et Automatica*, no. 2, pp. 98–102, 2022.
[22] H. Mehmet Baskonus, W. Gao, H. Rezazadeh et al., "New classifications of nonlinear Schrödinger model with group velocity dispersion via new extended method," *Results in Physics*, vol. 31, Article ID 104910, 2021.
[23] M. Arfan, K. Shah, A. Ullah, M. Shutaywi, P. Kumam, and Z. Shah, "On fractional order model of tumor dynamics with drug interventions under nonlocal fractional derivative," *Results in Physics*, vol. 21, Article ID 103783, 2021.
[24] M. Gubes, H. A. Peker, and G. Oturanç, "Application of differential transform method for el nino southern oscillation (enso) model with compared adomian decomposition and variational iteration methods," 2013, https://arxiv.org/abs/1307.7514.
[25] S. Liao and S. Sherif, "Beyond perturbation: introduction to the homotopy analysis method," *Applied Mechanics Reviews*, vol. 57, no. 5, pp. B25–B26, 2004.
[26] S. Liao, "Homotopy analysis method: a new analytical technique for nonlinear problems," *Communications in Nonlinear Science and Numerical Simulation*, vol. 2, pp. 95–100, 1997.
[27] H. Rezazadeh, M. Odabasi, K. U. Tariq, R. Abazari, and H. M. Baskonus, "On the conformable nonlinear Schrödinger equation with second order spatiotemporal and group velocity dispersion coefficients," *Chinese Journal of Physics*, vol. 72, pp. 403–414, 2021.
[28] M. Hosen, M. Chowdhury, M. Ali, and A. Ismail, "A new analytical technique for solving nonlinear non-smooth oscillators based on the rational harmonic balance method," *Proceedings of the Second International Conference on the Future of ASEAN (ICoFA) 2017–Volume 2*, pp. 453–463, Springer, Singapore, 2018.
[29] S. Ganji, D. D. Ganji, A. Davodi, and S. Karimpour, "Analytical solution to nonlinear oscillation system of the motion of a rigid rod rocking back using max–min approach," *Applied Mathematical Modelling*, vol. 34, no. 9, pp. 2676–2684, 2010.
[30] M. Mohammadian, "Nonlinear free vibration of damped and undamped bi-directional functionally graded beams using a cubic-quintic nonlinear model," *Composite Structures*, vol. 255, Article ID 112866, 2021.
[31] G. Sobamowo and A. Yinusa, "Power series-aftertreatment technique for nonlinear cubic duffing and double-well duffing oscillators," *Journal of Computational and Applied Mechanics*, vol. 48, pp. 297–306, 2017.
[32] M. Farhan, Z. Omar, F. Mebarek-Oudina et al., "Implementation of the one-step one-hybrid block method on the nonlinear equation of a circular sector oscillator," *Computational Mathematics and Modeling*, vol. 31, no. 1, pp. 116–132, 2020.
[33] Z. Y. Ren, "The frequency-amplitude formulation with ω4 for fast insight into a nonlinear oscillatorω4 for fast insight into a nonlinear oscillator," *Results in Physics*, vol. 11, pp. 1052-1053, 2018.
[34] H. L. Zhang, "Application of He's amplitude–frequency formulation to a nonlinear oscillator with discontinuity," *Computers & Mathematics with Applications*, vol. 58, no. 11-12, pp. 2197-2198, 2009.
[35] S. A. Pasha, Y. Nawaz, and M. S. Arif, "The modified homotopy perturbation method with an auxiliary term for the nonlinear oscillator with discontinuity," *Journal of Low Frequency Noise, Vibration and Active Control*, vol. 38, no. 3-4, pp. 1363–1373, 2019.
[36] A. Beléndez, C. Pascual, M. Ortuño, T. Beléndez, and S. Gallego, "Application of a modified He's homotopy perturbation method to obtain higher-order approximations to a nonlinear oscillator with discontinuities," *Nonlinear Analysis: Real World Applications*, vol. 10, no. 2, pp. 601–610, 2009.
[37] S. E. Ghasemi, A. Zolfagharian, and D. Ganji, "Study on motion of rigid rod on a circular surface using MHPM," *Propulsion and Power Research*, vol. 3, pp. 159–164, 2014.
[38] H. E. Khah and D. Ganji, "A study on the motion of a rigid rod rocking back and cubic-quintic duffing oscillators by using He's energy balance method," *International Journal of Nonlinear Science*, vol. 10, pp. 447–451, 2010.
[39] G. Sheng and X. Wang, "The dynamic stability and nonlinear vibration analysis of stiffened functionally graded cylindrical shells," *Applied Mathematical Modelling*, vol. 56, pp. 389–403, 2018.
[40] H. Ahmadi and K. Foroutan, "Nonlinear vibration of stiffened multilayer FG cylindrical shells with spiral stiffeners rested on damping and elastic foundation in thermal environment," *Thin-Walled Structures*, vol. 145, Article ID 106388, 2019.
[41] Y. Khan, Q. Wu, H. Askari, Z. Saadatnia, and M. Kalami-Yazdi, "Nonlinear vibration analysis of a rigid rod on a circular surface via Hamiltonian approach," *Mathematical and Computational Applications*, vol. 15, no. 5, pp. 974–977, 2010.
[42] M. Abul-Ez, G. M Ismail, and M. M El-Moshneb, "Analytical solutions for free vibration of strongly nonlinear oscillators," *Information Sciences Letters*, vol. 4, p. 7, 2015.
[43] N. A. Khan, M. Sulaiman, A. J. Aljohani, M. A. Bakar, and Miftahuddin, "Mathematical models of CBSC over wireless channels and their analysis by using the LeNN-WOA-NM

algorithm," *Engineering Applications of Artificial Intelligence*, vol. 107, Article ID 104537, 2022.

[44] N. A. Khan, M. Sulaiman, P. Kumam, and F. K. Alarfaj, "Application of Legendre polynomials based neural networks for the analysis of heat and mass transfer of a non-Newtonian fluid in a porous channel," *Advances in Continuous and Discrete Models*, vol. 2022, pp. 7–32, 2022.

[45] N. A. Khan, M. Sulaiman, C. A. Tavera Romero, and F. S. Alshammari, "Analysis of nanofluid particles in a duct with thermal radiation by using an efficient metaheuristic-driven approach," *Nanomaterials*, vol. 12, no. 4, p. 637, 2022.

[46] M. Rooman, M. A. Jan, Z. Shah, P. Kumam, and A. Alshehri, "Entropy optimization and heat transfer analysis in MHD Williamson nanofluid flow over a vertical Riga plate with nonlinear thermal radiation," *Scientific Reports*, vol. 11, pp. 18386–18414, 2021.

[47] N. A. Khan, M. Sulaiman, C. A. Tavera Romero, G. Laouini, and F. S. Alshammari, "Study of rolling motion of ships in random beam seas with nonlinear restoring moment and damping effects using neuroevolutionary technique," *Materials*, vol. 15, no. 2, p. 674, 2022.

[48] N. A. Khan, M. Sulaiman, P. Kumam, and A. J. Aljohani, "A new soft computing approach for studying the wire coating dynamics with Oldroyd 8-constant fluid," *Physics of Fluids*, vol. 33, no. 3, Article ID 036117, 2021.

[49] J. Lu, L. Ma, and Y. Sun, "Analysis of the nonlinear differential equation of the circular sector oscillator by the global residue harmonic balance method," *Results in Physics*, vol. 19, Article ID 103403, 2020.

[50] H. Mirgolbabaee, S. Tahernejad Ledari, N. Mohammad Zadeh, and D. Domiri Ganji, "Investigation of the nonlinear equation of the circular sector oscillator by Akbari-Ganji's method," *Journal of Taibah University for Science*, vol. 11, no. 6, pp. 1110–1121, 2017.

[51] X. Du, K. Farrahi, and M. Niranjan, "Transfer learning across human activities using a cascade neural network architecture," in *Proceedings of the 23rd international symposium on wearable computers*, pp. 35–44, London, U.K, September 2019.

[52] B. Warsito, R. Santoso, H. Yasin, and Suparti, "Cascade forward neural network for time series prediction," *Journal of Physics: Conference Series*, vol. 1025, Article ID 012097, 2018.

[53] Y. Zhang, J. Lin, Z. Hu, N. A. Khan, and M. Sulaiman, "Analysis of third-order nonlinear multi-singular emden–fowler equation by using the LeNN-WOA-NM algorithm," *IEEE Access*, vol. 9, pp. 72111–72138, 2021.